

Conformal mapping of rectangular heptagons

A. B. Bogatyrev

Abstract. A new effective approach to calculating the direct and inverse conformal mapping of rectangular polygons onto a half-plane is put forward; it is based on the use of Riemann theta functions.

Bibliography: 14 titles.

Keywords: Christoffel-Schwarz integral, Riemann surface, Jacobian, Siegel space, theta functions.

§ 1. Introduction

There exists an impressive list of numerical methods for conformal mapping of (simply connected) polygons [1]. A simple observation allows one to extend this list. Once the angles of the polygon are rational multiples of π , the Christoffel-Schwarz (CS) integral which maps the upper half-plane \mathbb{H} to the polygon is an Abelian integral on a compact Riemann surface. The full power of the function theory on Riemann surfaces may be applied now to attack the evaluation of the integral as well as its auxiliary parameters.

In this paper we consider a simply connected polygon with six right angles and one zero angle. This is the simplest case beyond the elliptic CS-integral (4 right angles in the polygon), described in [12]. We give the representation for both mappings: heptagon to the half-plane and back, as certain explicit expressions in terms of genus-two Riemann theta functions. For the latter there exist robust and effective methods of computation [3] with controllable accuracy. Therefore we can guarantee the machine accuracy for the conformal mapping uniformly in the polygon/half-plane.

As usual, there are several auxiliary parameters of the mapping which are determined by the geometrical dimensions of the polygon. Many problems, for instance, in classical mechanics, become simpler when written in a suitable system of coordinates. We shall see that this also holds for problems relating to conformal mappings: a good portion of those determining equations are linear if entries of the period matrix are taken for independent coordinates. Say, if we map an L -shaped rectangular hexagon, we have to solve just one nonlinear equation to determine the mapping.

This research was carried out with the support of the Russian Foundation for Basic Research (grant no. 10-01-00407) and the programme of the Department of Mathematical Sciences of the Russian Academy of Sciences “Modern Problems in Theoretical Mathematics”.

AMS 2010 Mathematics Subject Classification. Primary 14H42, 30A24, 30A28; Secondary 14H15.

This method may be used as a reference for testing numerical conformal mappings. It works equally well for the nonconvex polygons, in the presence of spikes of the boundary, narrow isthmuses, boundary elements of different scales, etc. This method enables an effective solution of boundary-value problems for harmonic functions, which can be, for example, the potentials of electric and magnetic fields, the stream and pressure functions in the flow of an ideal fluid, and so on. Furthermore, explicit analytic formulae for maps allow one to approach the problem of the design of domains: obtaining physical fields with required properties by selecting suitable geometric parameters. For instance, one can place the jet-separation point at a prescribed boundary point of the domains. Such problems are difficult to solve by standard numerical methods.

The author thanks the participants of the seminar on complex analysis at the Mathematical Institute of the Russian Academy of Sciences for their discussions of his work, V. Z. Ènol'skiĭ, who read the first version of the paper, for his useful suggestions, and O. A. Grigor'ev, who has put Fig. 1 at the author's disposal, for numerical computations.

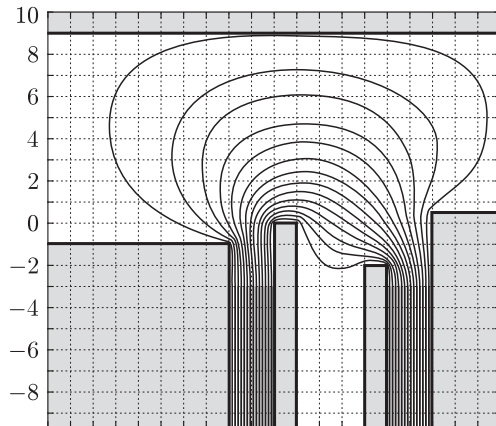


Figure 1. Flow pattern of an ideal fluid calculated by means of genus-two theta functions.

§ 2. The space of rectangular heptagons

We consider a rectangular heptagon with half-infinite, width- π ‘channel’ oriented to the east as shown in Fig. 2. Its sides are either vertical or horizontal. Two of the six right angles of the polygon must be intruding, that is, equal to $3\pi/2$, and the vertex with zero angle lies at infinity. The vertex at infinity is denoted by w_0 , the others are enumerated in increasing order with respect to the natural orientation of the boundary (counterclockwise). The two vertices with angles $3\pi/2$ are given special names w_α and w_β , $1 \leq \alpha < \beta \leq 6$.

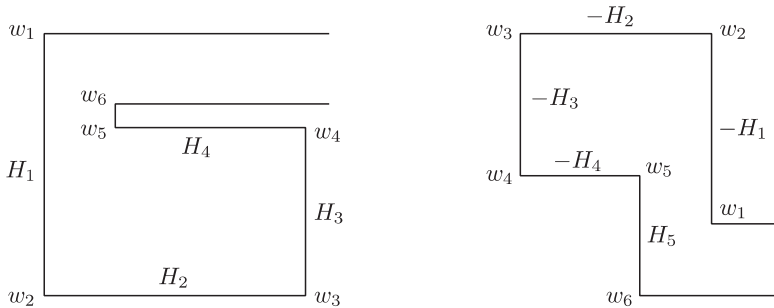


Figure 2. Heptagons from the spaces \mathcal{P}_{56} (left) and \mathcal{P}_{15} (right).

The space $\mathcal{P}_{\alpha\beta}$ of heptagons with fixed indices α and β is parametrized by the lengths of the sides, to which we ascribe signs for technical reasons:

$$i^s H_s := w_s - w_{s+1}, \quad s = 1, 2, \dots, 5. \quad (2.1)$$

One obvious restriction on the real quantities H_1, \dots, H_5 is as follows:

$$H_1 - H_3 + H_5 = \pi \quad (=:\text{Im}(w_1 - w_6)). \quad (2.2)$$

The sign of H_s is negative if and only if $\alpha \leq s < \beta$:

$$\left(s + \frac{1}{2} - \alpha\right) \left(s + \frac{1}{2} - \beta\right) H_s > 0. \quad (2.3)$$

The boundary of the heptagon has no self-intersections, which means that the dimensions obey the following additional inequalities:

(α, β)	Restrictions
(1, 2)	$-H_2 + H_4 > 0$
(1, 5)	$-H_2 + H_4 > 0$ when $H_1 - H_3 \leq 0$
(2, 3)	$-H_3 + H_5 > 0$
(2, 6)	$-H_2 + H_4 < 0$ when $-H_3 + H_5 \leq 0$
(4, 5)	$H_1 - H_3 > 0$
(5, 6)	$-H_2 + H_4 < 0$

Lemma 1. *The heptagons with fixed indexes α and β make up a connected space $\mathcal{P}_{\alpha\beta}$ of real dimension 4 with the global coordinates H_1, \dots, H_5 subject to restriction (2.2), the sign rule (2.3) and inequalities (2.4).*

A point in the space $\mathcal{P}_{\alpha,\beta}$ defines a heptagon up to translations in the plane only. Those translations may be eliminated when necessary by normalization: for example, $w_1 := i\pi$. The reflection in the real axis induces the mapping $\mathcal{P}_{\alpha,\beta} \rightarrow \mathcal{P}_{7-\beta,7-\alpha}$, which in the above coordinate system appears as

$$(H_1, H_2, \dots, H_5) \rightarrow (H_5, H_4, \dots, H_1).$$

§ 3. Hyperelliptic curves with six real branch points

The conformal mapping of the upper half-plane to any heptagon from the space $\mathcal{P}_{\alpha\beta}$ may be represented by the Christoffel-Schwarz integral. This integral lives on a hyperelliptic curve with six real branch points, which are inverse images of right-angled vertices. In this section we briefly recall several facts about such curves.

3.1. Algebraic model. The double cover of the sphere with six real branch points $x_1 < x_2 < \dots < x_5 < x_6$ is a compact genus-two Riemann surface X with the equation (of its affine part):

$$y^2 = \prod_{s=1}^6 (x - x_s), \quad (x, y) \in \mathbb{C}^2. \quad (3.1)$$

This curve admits a conformal involution $J(x, y) = (x, -y)$ with six stationary points $p_s := (x_s, 0)$ and an anticonformal involution (reflection) $\bar{J}(x, y) = (\bar{x}, \bar{y})$. The stationary-point set of the latter has three components known as *real ovals* of the curve. Each real oval is an embedded circle and doubly covers exactly one of the segments $[x_2, x_3]$, $[x_4, x_5]$ and $[x_6, x_1] \ni \infty$ of the extended real line $\mathbb{R} := \mathbb{R} \cup \infty$. We call these ovals *first*, *second* and *third*, respectively. The lift of the complementary set of intervals $[x_1, x_2]$, $[x_3, x_4]$, $[x_5, x_6]$ to the surface (3.1) gives us three *coreal ovals*, which make up the set of points fixed by another anticonformal involution $\bar{J}J = J\bar{J}$.

3.2. Cycles, differentials and periods. We fix a special basis in the 1-homology space of the curve X uniquely determined by the latter. The first and second real ovals give us two 1-cycles, a_1 and a_2 , respectively. Both cycles are oriented (up to simultaneous change of sign) as the boundary of a pair of pants obtained by removing real ovals from the surface (3.1). The two remaining cycles b_1 and b_2 are coreal ovals of the curve oriented so that the intersection matrix takes the canonical form, see Fig. 3.

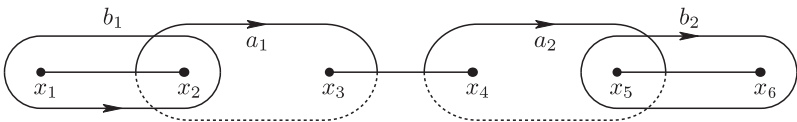


Figure 3. Canonical basis in the homologies of the curve X .

The reflection of the surface acts on the introduced basis as follows:

$$\bar{J}a_s = a_s, \quad \bar{J}b_s = -b_s, \quad s = 1, 2. \quad (3.2)$$

Holomorphic differentials on the curve X take the form

$$du_* = (C_{1*}x + C_{2*}) \frac{dx}{y} \quad (3.3)$$

with constant quantities C_{1*} and C_{2*} . The basis of differentials dual to the basis of cycles is defined by

$$\int_{a_s} du_j := \delta_{sj}, \quad s, j = 1, 2, \quad (3.4)$$

and determines the Riemann period matrix Π with the elements

$$\Pi_{sj} := \int_{b_s} du_j, \quad s, j = 1, 2. \quad (3.5)$$

It is Riemann's classical result that Π is symmetric and has positive-definite imaginary part [4].

From the symmetry properties (3.2) of the chosen basic cycles it readily follows that:

- normalized differentials are real, that is, $\bar{J}du_s = \overline{du_s}$; in other words the coefficients C_* in the representation (3.3) are real;
- the period matrix is purely imaginary, therefore we can introduce the symmetric and positive-definite real matrix $\Omega := \text{Im}(\Pi)$;
- zeros of the differential du_2 (resp. du_1) lie on the first (resp. second) real oval of the curve.

3.3. Jacobian and Abel-Jacobi map.

Definition 1. Given a Riemann period matrix Π , we define the full-rank lattice

$$L(\Pi) = \Pi\mathbb{Z}^2 + \mathbb{Z}^2 = \int_{H_1(X, \mathbb{Z})} du, \quad du := (du_1, du_2)^t \quad (3.6)$$

in \mathbb{C}^2 and the 4-torus $\text{Jac}(X) := \mathbb{C}^2/L(\Pi)$, known as the Jacobian of the curve X .

Of course, this definition depends on the choice of the basis in the integer homology lattice $H_1(X, \mathbb{Z})$; other choices bring us to isomorphic tori.

It is convenient to represent points $u \in \mathbb{C}^2$ as a theta characteristic $[\varepsilon, \varepsilon']$, that is, a couple of real 2-vectors (columns) $\varepsilon, \varepsilon'$ of height $g = 2$:

$$u = \frac{1}{2}(\Pi\varepsilon + \varepsilon'). \quad (3.7)$$

Points in the Jacobian $\text{Jac}(X)$ in this notation correspond to two vectors with real entries modulo 2. Second-order points of the Jacobian are represented as 2×2 matrices with \mathbb{Z}_2 entries. Please note that we use a nonstandard notation of the theta characteristic as two column vectors written one after another. Usually the transposed matrix is used.

Definition 2. The Abel-Jacobi (briefly AJ) map $X \rightarrow \text{Jac}(X)$ is defined by the formula

$$u(p) := \int_{p_1}^p du \pmod{L(\Pi)}, \quad p_1 := (x_1, 0), \quad du := (du_1, du_2)^t. \quad (3.8)$$

Sometimes the AJ map is considered as acting from the universal covering space of X into \mathbb{C}^2 . From the Riemann-Roch formula it easily follows [4] that the Abel-Jacobi map is a holomorphic embedding of the curve into its Jacobian.

In § 5 we give an explicit equation for the image of the genus-two curve in its Jacobian. Let us meanwhile compute the images of the branching points $p_s = (x_s, 0)$, $s = 1, \dots, 6$ of the curve X :

p	$u(p) \bmod L(\Pi)$	$[\varepsilon, \varepsilon'](u(p))$
p_2	$\frac{\Pi^1}{2}$	$\begin{bmatrix} 1 & 0 \\ 0 & 0 \end{bmatrix}$
p_3	$\frac{\Pi^1 + E^1}{2}$	$\begin{bmatrix} 1 & 1 \\ 0 & 0 \end{bmatrix}$
p_4	$\frac{\Pi^2 + E^1}{2}$	$\begin{bmatrix} 0 & 1 \\ 1 & 0 \end{bmatrix}$
p_5	$\frac{\Pi^2 + E^1 + E^2}{2}$	$\begin{bmatrix} 0 & 1 \\ 1 & 1 \end{bmatrix}$
p_6	$\frac{E^1 + E^2}{2}$	$\begin{bmatrix} 0 & 1 \\ 0 & 1 \end{bmatrix}$

Here Π^s and E^s are the s th columns of the period- and identity-matrix, respectively. One can notice that the vector $\varepsilon(u(p))$ is constant along the real ovals and $\varepsilon'(u(p))$ is constant along the coreal ovals.

3.4. Tiling the Jacobian. The Jacobian is the closure of the union of 16 disjoint blocks (tiles) filled by the points with theta characteristics in the sets

$$\begin{bmatrix} \pm I & \pm I \\ \pm I & \pm I \end{bmatrix}, \quad I := (0, 1),$$

distinguished by the possible choices of four signs.

Having chosen an orientation on a real oval of the curve, one can distinguish a component in the set $x^{-1}\mathbb{H} \subset X$ which lies to the left of this oval. We shall denote this disc by \mathbb{H}^+ . The surface X with all real and coreal ovals removed is a disjoint union of four open 2-discs \mathbb{H}^+ , $J\mathbb{H}^+$, $\bar{J}\mathbb{H}^+$, $\bar{J}J\mathbb{H}^+$. It turns out that the AJ map sends each of these discs to a certain block of the Jacobian and each (co)real oval to a certain 2-torus. This helps us to discriminate points $p \in X$ with the same value of the projection $x(p)$.

Theorem 1. *Let the disc \mathbb{H}^+ be chosen in accordance with the orientation of (any of) the a -cycles. Then the above four discs are mapped by the AJ mapping to the following four blocks of the Jacobian:*

$p \in$	\mathbb{H}^+	$J\mathbb{H}^+$	$\bar{J}\mathbb{H}^+$	$\bar{J}J\mathbb{H}^+$
$[\varepsilon, \varepsilon'](u(p)) \in$	$\begin{bmatrix} -I & I \\ -I & I \end{bmatrix}$	$\begin{bmatrix} I & -I \\ I & -I \end{bmatrix}$	$\begin{bmatrix} I & I \\ I & I \end{bmatrix}$	$\begin{bmatrix} -I & -I \\ -I & -I \end{bmatrix}$

Proof. Symmetries of the normalized Abelian differentials with respect to the involutions J, \bar{J} guarantee the following equalities: $u(Jp) = -u(p)$; $u(\bar{J}p) = \overline{u(p)}$ since the base point p_1 of the AJ map is fixed by both involutions. Therefore we may thoroughly investigate the map on the disc \mathbb{H}^+ only.

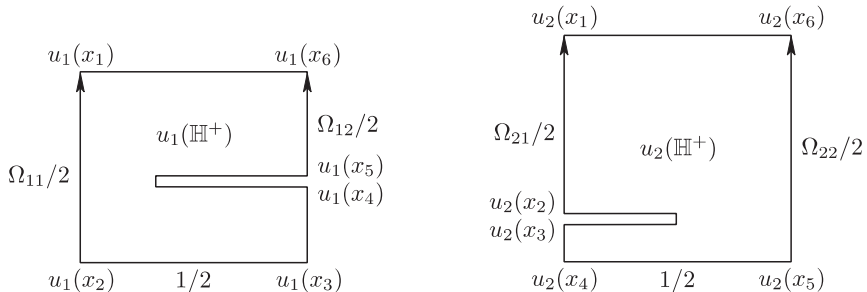


Figure 4. The images of the upper half-plane $u_1(\mathbb{H}^+)$ (left) and $u_2(\mathbb{H}^+)$ (right).

Both components $u_s(p)$ of the Abel-Jacobi map are CS integrals and send the disc \mathbb{H}^+ to the rectangles with slots shown in Fig. 4. Clearly, the real part of $u_s(p)$ lies in the interval $(0, 1/2)$ which may be reformulated as $\varepsilon'(u(p)) \in (I, I)^t$.

To study the range of the 2-vector $\varepsilon := 2\Omega^{-1} \text{Im } u(p)$ we introduce the new differentials

$$dv = (dv_1, dv_2)^t := -i\Omega^{-1} du.$$

These are purely imaginary with normalization $\int_{b_j} dv_s = \delta_{js}$. The differential dv_1 has zeros on the coreal oval covering the interval (x_5, x_6) ; dv_2 has zeros projecting on (x_1, x_2) . Again, each Abelian integral $v_s(p)$ maps the upper half-plane to the rectangle with slot similar to that in the left Fig. 4, but now the vertex $v_s(x_1)$ lies on the right side of the rectangle, therefore $\varepsilon(u(p)) := 2 \text{Re } v(p) \in (-I, -I)^t$.

§ 4. Two moduli spaces

We are going to describe the space of CS integrals corresponding to the rectangular heptagons from the space $\mathcal{P}_{\alpha\beta}$. This space is an extension of the underlying space of genus-2 curves with real branch points.

4.1. Genus-2 curves with three real ovals. Each genus-two curve X is automatically hyperelliptic, that is, it admits a conformal involution J that fixes six points. This involution is unique. The Riemann surface is said to have a reflection if it admits an anticonformal involution \bar{J} (the same surface X may have several reflections). Each component of the set of \bar{J} -fixed points is an embedded circle [5] known as a *real oval* of the reflection.

Definition 3. The moduli space $\mathcal{M}_2\mathbb{R}_3$ is the space of genus-two Riemann surfaces with reflection and three enumerated real ovals. Two surfaces are equivalent if there is a conformal 1 – 1 mapping between them commuting with the reflections and respecting the marking of real ovals.

Let us consider the constructive model of an element $X \in \mathcal{M}_2\mathbb{R}_3$. Necessarily, the involutions J and \bar{J} of X commute (otherwise J is not unique) and therefore \bar{J} acts on the Riemann sphere X/J . Once the reflection of the surface acts with fixed points, so does the induced reflection of the sphere. For a suitable choice of the global coordinate x on the sphere, the reflection of the latter works as complex conjugation. It is convenient to think of x as a degree-two meromorphic function on the surface. Obviously, it maps each real oval on X to the subset of the real equator $\widehat{\mathbb{R}} := \mathbb{R} \cup \infty$ of the Riemann sphere. There are three possibilities for the image of a real oval:

- (i) x maps the oval $1 - 1$ to the equator;
- (ii) the oval is mapped $2 - 1$ to the equator, or
- (iii) an oval is mapped $2 - 1$ to the finite segment of it.

In the latter case the end-points of the segment are the critical values of the projection x .

Simple combinatorial arguments show that in the case of three real ovals on X , they are projected to three nonoverlapping intervals of the real equator of the sphere. The end-points of those intervals are the projections of the stationary points of the involution J of the surface X . We can give them unique names in the following way.

Projections of the first, second and third ovals induce either the natural cyclic order of the real equator, or the inverse. In the latter case we change the sign of the coordinate x . Now we can enumerate the end-points of the intervals in the natural cyclic order as x_1, x_2, \dots, x_6 so that the first real oval of the surface is $x^{-1}([x_2, x_3])$, the second is $x^{-1}([x_4, x_5])$ and the third is $x^{-1}([x_6, x_1])$. Note that an interval of the extended real axis $\widehat{\mathbb{R}}$ may contain infinity as its interior or boundary point. We have shown that our first definition of the moduli space is equivalent to the following one.

Definition 4. The moduli space $\mathcal{M}_2\mathbb{R}_3$ is the factor of the cyclically ordered sextuples (x_1, \dots, x_6) from $\widehat{\mathbb{R}}$ modulo the action of $\mathrm{PSL}_2(\mathbb{R})$ (= real projective transformations conserving the orientation of the equator).

Normalizing the branch points, for example, as $x_4 = \infty$, $x_5 = -1$, $x_6 = 0$, one gets the global coordinate system on the moduli space:

$$0 < x_1 < x_2 < x_3 < \infty. \quad (4.1)$$

Other normalizations bring us to other global coordinate systems in the same space. Yet another global coordinate system in this space is related to the periods of holomorphic differentials.

Theorem 2. *The period mapping $\Omega(X)$ is a real analytic diffeomorphism from the moduli space $\mathcal{M}_2\mathbb{R}_3$ to the trihedral cone*

$$0 < \Omega_{12} < \min(\Omega_{11}, \Omega_{22}). \quad (4.2)$$

Proof. First of all, the matrix $\Omega := \mathrm{Im} \Pi$ is a well defined function on the moduli space: both choices of the intrinsic basis in the space of integer 1-cycles introduced in § 3.2 bring us to the same period matrix.

The CS integrals $u_j(x) := \int_{x_1}^x du_j$ map the upper half-plane $1-1$ to the rectangles with slots shown in Fig. 4. The dimensions of the rectangles are related to the elements of the period matrix, whence inequalities (4.2) follow.

Now we see that all the curves $X \in \mathcal{M}_2\mathbb{R}_3$ with fixed first column of the period matrix are parametrized by the length l of the slot in the left rectangle of Fig. 4. In particular, Ω_{22} is a monotonic function of l . Now one can study the asymptotic behaviour of this function and show that $\Omega_{22}(l) \rightarrow \infty$ as $l \rightarrow 0$ [6] and $\Omega_{22}(l) \rightarrow \Omega_{21}$ as $l \rightarrow 1$ [7].

Remark 1. The inverse mapping, from the period matrices to the (suitably normalized) branch points of the curve is also effective. For genus two it is implemented by the Rosenhain formulae [8] (see also §5) in terms of theta constants.

Remark 2. The cone (4.2) is strictly smaller than the space of all real positive-definite symmetric 2×2 matrices Ω . It is known (see, for instance, [9]) that any indecomposable matrix in the Siegel genus-two space is the period matrix of some Riemann surface. The decomposable matrices make up a component of the codimension-one Humbert variety which is determined by the vanishing of at least one of the 10 even theta constants. In our case of real curves the Humbert variety is a real codimension-one subvariety in the real 3-dimensional matrix space and its complement is disconnected. One can check that

$$\begin{aligned} \theta \begin{bmatrix} 1 & 1 \\ 1 & 1 \end{bmatrix} (i\Omega) &= 0 \text{ on the edge } \{\Omega_{12} = 0\} \text{ of the cone,} \\ \theta \begin{bmatrix} 0 & 1 \\ 1 & 0 \end{bmatrix} (i\Omega) &= 0 \text{ on the edge } \{\Omega_{12} = \Omega_{11}\} \text{ and} \\ \theta \begin{bmatrix} 1 & 0 \\ 0 & 1 \end{bmatrix} (i\Omega) &= 0 \text{ on the edge } \{\Omega_{12} = \Omega_{22}\}. \end{aligned}$$

The definitions of the theta constants will be given in §5.

4.2. Curves with a marked point on a real oval. The problems of conformal mapping use a slightly more sophisticated moduli space, that of the genus-two real curves with a marked point on a real oval (see, for instance, [10]).

Definition 5. The space of genus-two Riemann surfaces with three enumerated real ovals and a marked point $p_0 \neq Jp_0$ on the third oval we call $\mathcal{M}_{2,1}\mathbb{R}_3$. Two surfaces are equivalent if and only if there is a conformal mapping between them commuting with the reflections and respecting the enumeration of the ovals as well as the marked point.

An argument similar to that in §4.1 shows that we can introduce an equivalent but more constructive definition.

Definition 6. By $\mathcal{M}_{2,1}\mathbb{R}_3$ we mean the sets of seven cyclically ordered points (x_0, x_1, \dots, x_6) in the real equator $\widehat{\mathbb{R}}$ of the Riemann sphere modulo the action of $PSL_2(\mathbb{R})$. For brevity we call this the large moduli space.

Here x_0 means the projection of the marked point to the sphere, other coordinates are the projections of the branch points of the curve. The natural projection of $\mathcal{M}_{2,1}\mathbb{R}_3$ to the space $\mathcal{M}_2\mathbb{R}_3$ consists in forgetting the marked point x_0 .

Recall that for the element X of the space $\mathcal{M}_2\mathbb{R}_3$ there is no natural distinction between two components of the set $x^{-1}\mathbb{H} \subset X$ until we orient a real oval. The difference arises once we mark a point $p_0 \neq Jp_0$ on a real oval: there is a unique disc $\mathbb{H}^+ \subset x^{-1}\mathbb{H}$ with p_0 on its boundary.

One can introduce several coordinate systems on the space $\mathcal{M}_{2,1}\mathbb{R}_3$. Fixing three points of seven, say $x_4 := \infty$, $x_5 := -1$ and $x_6 := 0$, the positions of the remaining four points of the 7-tuple will give us the global coordinate system on the large moduli space:

$$0 < x_0 < x_1 < x_2 < x_3 < \infty. \quad (4.3)$$

Other normalizations of the 7-tuple of points result in different coordinate systems on the large moduli space. It is a good exercise to show that the arising coordinate change is a real analytic 1-1 mapping from the 4D cell (4.3) to the appropriate cell.

Yet another coordinate system on $\mathcal{M}_{2,1}\mathbb{R}_3$ is related to the period matrix. Three variables Ω_{11} , Ω_{12} , Ω_{22} are inherited from the space $\mathcal{M}_2\mathbb{R}_3$ and the fourth is either u_1^0 or u_2^0 , the component of the image of the marked point under the AJ map. The integration path for $u^0 = u(p_0)$ is the interval of the third real oval avoiding the branch point p_6 .

Lemma 2. *Each of the two mappings*

$$(x_0, x_1, x_2, x_3) \rightarrow (\Omega_{11}, \Omega_{12}, \Omega_{22}, u_s^0), \quad s = 1, 2,$$

is a real analytic diffeomorphism of the cone (4.3) to the product of the cone (4.2) and the interval $(0, 1/2)$.

Proof. Let us regard the points x_s , $s = 0, 1, 2, 3$ as the coordinates in the space $\mathcal{M}_{2,1}\mathbb{R}_3$, other branch points being fixed. By definition, the period matrix Ω is independent of the position of the marked point p_0 and the mapping $(x_1, x_2, x_3) \rightarrow \Omega$ is a real analytic diffeomorphism from the cell (4.1) to the cone (4.2). Both basic differentials du_1 and du_2 are real and have no zeros on the third real oval containing the marked point. Therefore, both quantities $u_s(p_0)$ increase monotonically from zero to $\frac{1}{2} = \frac{1}{2} \int_{a_1+a_2} du_s$ as the marked point p_0 moves from p_1 to p_6 along the third real oval.

The periods of more sophisticated differentials taken instead of du_s bring us to yet another coordinate system in the same moduli space of curves with marked points on them.

4.2.1. Christoffel-Schwarz differentials. Let $1 \leq \alpha < \beta \leq 6$ be a couple of integers labelling the spaces of heptagons. To each element of the moduli space $\mathcal{M}_{2,1}\mathbb{R}_3$ we ascribe the unique Abelian differential $dw_{\alpha\beta}$ of the third kind with simple poles at the points p_0 and Jp_0 , with residues resp. -1 and $+1$ at these points and zeros at the branch points p_α and p_β (one of the ways to normalize a meromorphic differential is to put its zeros at the points of a nonspecial degree- g divisor). The differential will automatically have double zeros because it is odd with respect to the involution J .

In the algebraic model (3.1) it takes the form

$$dw_{\alpha\beta} = (x - x_\alpha)(x - x_\beta) \frac{dx}{y}, \quad (4.4)$$

where $y^2 = \prod_{j=1}^6 (x - x_j)$ and the 7-tuple $\infty =: x_0, x_1, \dots, x_6$ represents an element of the space $\mathcal{M}_{2,1}\mathbb{R}_3$. The Christoffel-Schwarz differential (4.4) can be decomposed into a sum of three elementary ones:

$$dw_{\alpha\beta} = dv_{Jp_0p_0} + C_1 du_1 + C_2 du_2, \quad (4.5)$$

where dv_{rq} is an a -normalized third-kind Abelian differential with poles at r and q ; du_1 and du_2 form the basis of holomorphic differentials and the constants C_1 and C_2 are uniquely determined by the condition that $dw_{\alpha\beta}$ has zeros at the branching points p_α and p_β .

Each element of the heptagon space $\mathcal{P}_{\alpha\beta}$ is the image of the upper half-plane under the Christoffel-Schwarz map

$$w_{\alpha\beta}(x) := \int_*^x dw_{\alpha\beta}. \quad (4.6)$$

Actually, even more is true.

Theorem 3. *The Christoffel-Schwarz mapping $w_{\alpha\beta}(x)$ induces a real analytic diffeomorphic map from the moduli space $\mathcal{M}_{2,1}\mathbb{R}_3$ to the heptagon space $\mathcal{P}_{\alpha\beta}$.*

Proof. First of all we check that each CS differential is real: $\overline{J}dw_{\alpha\beta} = \overline{dw_{\alpha\beta}}$. This implies that the increment of the CS-map on the boundary of the disc \mathbb{H}^+ embedded in the Riemann surface is real on the real ovals and it is purely imaginary on the coreal ovals. This increment is monotonic between the branch points apart from a neighbourhood of p_0 . The image of $\partial\mathbb{H}^+$ under the CS-map is a polygonal line with the same sequence of corners as in any heptagon from the space $\mathcal{P}_{\alpha\beta}$; namely all the corners are equal to $\pi/2$ apart from those at p_α and p_β which are equal to $3\pi/2$. Moreover, this polygonal line has no self-intersections. For instance, in the case $(\alpha, \beta) = (2, 6)$ the self-intersection shown in Fig. 5 is impossible because the points of the rectangle marked by $*$ have -1 preimages in \mathbb{H}^* according to the argument principle.

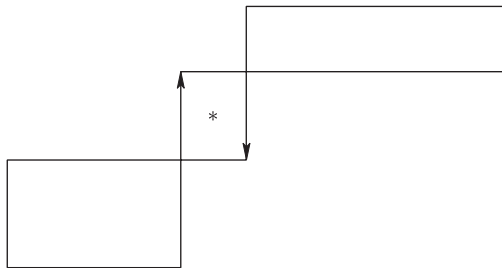


Figure 5. Self-intersection of the image of the real equator under the map w_{26} .

We have established a 1 – 1 correspondence between the large moduli space and the space of heptagons induced by the CS-map (4.6). One can easily see that the dimensions of the heptagon (that is, the coordinates in the space $\mathcal{P}_{\alpha\beta}$) are the periods of the corresponding CS-integral:

$$\begin{aligned} iH_1 &:= \int_{p_2}^{p_1} dw_{\alpha\beta} = \frac{1}{2} \int_{b_1} dw_{\alpha\beta}, & i^2H_2 &:= \int_{p_3}^{p_2} dw_{\alpha\beta} = -\frac{1}{2} \int_{a_1} dw_{\alpha\beta}, \\ i^3H_3 &:= \int_{p_4}^{p_3} dw_{\alpha\beta} = i\pi + \frac{1}{2} \int_{b_2-b_1} dw_{\alpha\beta}, & & (4.7) \\ i^4H_4 &:= \int_{p_5}^{p_4} dw_{\alpha\beta} = -\frac{1}{2} \int_{a_2} dw_{\alpha\beta}, & i^5H_5 &:= \int_{p_6}^{p_5} dw_{\alpha\beta} = \frac{1}{2} \int_{-b_2} dw_{\alpha\beta}. \end{aligned}$$

Now we prove the real analyticity of the direct and inverse mappings.

The basic 1-cycles may be separated from the branch points of the surface, so the real analyticity of the direct map $\mathcal{M}_{2,1}\mathbb{R}_3 \rightarrow \mathcal{P}_{\alpha\beta}$ is clear. It remains to show that the map has full rank.

Let us consider the coordinate system in the large moduli space such that $x_0 = \infty$, $x_\alpha = -1$, $x_\beta = 1$. Assume that the CS-induced map degenerates at a point (x_0, x_1, \dots, x_6) of the large moduli space; then there exists a nontrivial tangent vector $\xi := \sum_{1=j \notin \{\alpha, \beta\}}^6 \xi_j \frac{\partial}{\partial x_j}$ annihilating all the periods of the CS-differential $dw_{\alpha\beta}$ at this point. This means the existence of a meromorphic differential

$$dv := \frac{1}{2} \sum_{1=j \notin \{\alpha, \beta\}}^6 \xi_j \frac{dw_{\alpha\beta}}{x - x_j}$$

with zero cyclic and polar periods on the associated surface and with poles at the branch points of the surface, except p_α and p_β . Then the meromorphic function

$v(x, y) := \int_{p_\alpha}^{(x, y)} dv$ is single valued on the surface and has at most four simple poles along with triple zeros at the points p_α and p_β (since $\int_\alpha^\beta dv = 0$). Such a function is identically equal to zero and therefore the above tangent vector is also zero. Hence the CS-induced mapping $\mathcal{M}_{2,1}\mathbb{R}_3 \rightarrow \mathcal{P}_{\alpha\beta}$ has full rank everywhere.

4.2.2. Auxiliary parameters of the CS-map. Given a heptagon from the space $\mathcal{P}_{\alpha\beta}$, the corresponding point in the moduli space $\mathcal{M}_{2,1}\mathbb{R}_3$ may be found as a (unique, as follows from Theorem 3) solution of the following system of equations obtained from (4.7) by substituting the decomposition (4.5) of the Christoffel-Schwarz differential into elementary differentials:

$$\begin{aligned} 2H_1 &= (C_1\Omega_{11} + C_2\Omega_{12} + 2\pi(1 - 2u_1^0)), \\ 2H_2 &= C_1, \\ 2H_4 &= -C_2, \\ 2H_5 &= -(C_1\Omega_{12} + C_2\Omega_{22} - 4\pi u_2^0). \end{aligned} \tag{4.8}$$

(We have also used the Riemann bilinear relations (5.11) to transform the b -periods of the elementary differential of the 3-rd kind to the Abel-Jacobi image of its polar divisor.) Here C_1 and C_2 are the real analytic functions on the moduli space defined above as a solution of a linear system with the nonsingular 2×2 matrix $\|du(p_\alpha), du(p_\beta)\|$. We see that the auxiliary system of equations is ‘almost linear’ with respect to the coordinate system related to the periods of holomorphic differentials. It remains to get the effective evaluation of the functions C_1, C_2 and u_2^0 as well as the CS-integral itself. This is the subject of the next section.

§ 5. Theta functions on genus-two surfaces

Here we give a short introduction to the theory of Riemann theta functions adapted to genus-two surfaces. Three problems related to conformal mappings will be effectively solved in terms of Riemann theta functions:

- localization of the AJ-image of a curve inside its Jacobian;
- representation of the 2-sheeted projection of a curve onto the sphere;
- evaluation of the normalized Abelian integral of the third kind (which is the essential part of the CS-integral).

Definition 7. Let $u \in \mathbb{C}^2$ and let $\Pi \in \mathbb{C}^{2 \times 2}$ be a Riemann matrix, that is, $\Pi = \Pi^t$ and $\text{Im } \Pi > 0$. The theta function of these two arguments is the following Fourier series:

$$\theta(u, \Pi) := \sum_{m \in \mathbb{Z}^2} \exp(2\pi i m^t u + \pi i m^t \Pi m). \quad (5.1)$$

Authors also consider theta functions with characteristics, which are a slight generalization of the theta function defined above:

$$\begin{aligned} \theta[2\varepsilon, 2\varepsilon'](u, \Pi) &:= \sum_{m \in \mathbb{Z}^2} \exp(2\pi i(m + \varepsilon)^t(u + \varepsilon') + \pi i(m + \varepsilon)^t \Pi(m + \varepsilon)) \\ &= \exp(i\pi \varepsilon^t \Pi \varepsilon + 2i\pi \varepsilon^t(u + \varepsilon')) \theta(u + \Pi \varepsilon + \varepsilon', \Pi), \quad \varepsilon, \varepsilon' \in \mathbb{R}^2. \end{aligned} \quad (5.2)$$

The matrix argument Π of the theta function is usually omitted when it is clear which matrix we mean. An omitted vector argument u is supposed to be zero and the appropriate function of Π is called the theta constant. The omitted vector argument u is supposed to be zero and the resulting function of Π is called the theta constant:

$$\theta[\varepsilon, \varepsilon'] := \theta[\varepsilon, \varepsilon'](0, \Pi).$$

The series under consideration have a high convergency rate since the matrix $\text{Im } \Pi$ is positive-definite, and the remainder term is easy to estimate [3]. Theta functions have the following easily checked quasi-periodicity evenness (or oddness) properties with respect to the lattice $L(\Pi) := \Pi \mathbb{Z}^2 + \mathbb{Z}^2$.

Lemma 3 (see [11], [12]). (i) For $m, m' \in \mathbb{Z}^2$ and $\varepsilon, \varepsilon' \in \mathbb{R}^2$

$$\theta[\varepsilon, \varepsilon'](u + \Pi m + m', \Pi) = \exp(-i\pi(m^t \varepsilon' - \varepsilon^t m' + m^t \Pi m + 2m^t u)) \theta[\varepsilon, \varepsilon'](u, \Pi). \quad (5.3)$$

(ii) For $\varepsilon, \varepsilon' \in \mathbb{Z}^2$

$$\theta[\varepsilon, \varepsilon'](-u, \Pi) = (-1)^{\varepsilon^t \cdot \varepsilon'} \theta[\varepsilon, \varepsilon'](u, \Pi). \quad (5.4)$$

Correspondingly, the integer theta characteristic $[\varepsilon, \varepsilon']$ is said to be even or odd depending on the parity of the scalar product $\varepsilon^t \cdot \varepsilon'$.

In particular, it follows from (5.3) that the zero set of the theta function is a well defined subset of the Jacobian. The Abel-Jacobi map transfers the theta function to the Riemann surface where it becomes the multivalued function (or a section of a certain line bundle)

$$\theta_e(p) := \theta(u(p) - e; \Pi), \quad e \in \mathbb{C}^2,$$

which is multiplied by some nonvanishing factors once its argument p goes around handles of the surface. Therefore, its zeros are well defined. The zero set of the theta function is described by the so called Riemann vanishing theorems the most important of which is as follows [4], [11], [12].

Theorem 4 (Riemann). *A function $\theta_e(p)$ on a genus-two surface either*

- (i) *vanishes identically on the surface if and only if e is a certain effectively calculated point K of the Jacobian (a.k.a. the vector of Riemann constants), or*
- (ii) *has exactly two zeros q_1, q_2 such that $q_1 \neq Jq_2$ and*

$$e = u(q_1) + u(q_2) + K \pmod{L(\Pi)}. \quad (5.5)$$

5.1. Vector of Riemann constants. We have to determine the vector of Riemann constants K for our particular choice of the initial point in the AJ-map and the choice of the basis in the homologies.

Lemma 4. *The vector of Riemann constants has the representation*

$$K = u(p_3) + u(p_5). \quad (5.6)$$

Proof. We see from the table in §3.3 that the points p_3 and p_5 correspond to odd characteristics. Relation (5.4) implies that the function $\theta(u(p))$ will have zeros at the points $p = p_3, p_5$ on the surface. This function cannot be identically zero on the surface: otherwise from part (i) of the Riemann vanishing theorem it would follow that $K = 0$. Now one can check that the function $\theta_e(p)$ with the shift $e := u(p_3) + u(p_5) + K$ is not identically zero (since $p_3 \neq Jp_5$) and vanishes at the three points $p = p_1, p_3, p_5$.

Alternative (ii) of the Riemann vanishing Theorem 4 suggests that

$$K = u(p_3) + u(p_5) \pmod{L(\Pi)}.$$

In other words, K corresponds to the odd characteristics $\begin{bmatrix} 10 \\ 11 \end{bmatrix}$.

Remark 3. It is convenient to represent integer theta characteristics as the sums of AJ-images of the branch points, keeping only the indices of these points: $[sk \dots l]$ means the sum modulo 2 of the theta characteristics of points $u(p_s), u(p_k), \dots, u(p_l)$, for example, [35] is the vector of Riemann constants represented by theta characteristics.

5.2. Image of the Abel-Jacobi map. The location of a genus-2 curve embedded in its Jacobian may be reconstructed by solving a single equation.

Theorem 5 (Riemann). *A point e of the Jacobian lies in the image $u(X)$ of the Abel-Jacobi map if and only if*

$$\theta \begin{bmatrix} 1 & 0 \\ 1 & 1 \end{bmatrix} (e) = 0.$$

Proof. 1. The function $\theta(u(p) - K)$ vanishes identically on the curve and hence so does the function $\theta[35](u(p))$ by Theorem 4.

2. Conversely, suppose that $\theta[35](e) = 0$ or equivalently, $\theta(e + K) = 0$. The function $\theta_{e'}(p)$ with the shift $e' := e + K$ either vanishes at two points p_1, p' and in this case $e = u(p')$, or vanishes identically, then $e = 0 = u(p_1)$.

5.3. Projection onto the sphere. Any meromorphic function on the curve may be effectively calculated via the Riemann theta functions once we know its divisor. Take for instance the degree-2 function x on the hyperelliptic curve (3.1). This function is unique if normalized, for instance, as follows: $x(p_s) = 0$, $x(p_j) = 1$, $x(p_l) = \infty$, where s, j, l is a positive triple from the index set $\{1, 2, \dots, 6\}$.

With the use of the transformation rules (5.3) one immediately checks that the following function is single-valued on the curve:

$$\tilde{x}(p) := \frac{\theta^2[sk35](u(p), \Pi)}{\theta^2[lk35](u(p), \Pi)}, \quad k \neq s, l.$$

Now with the help of Theorem 4 one checks that the numerator of the function has double zeros at the points p_s, p_k while the denominator has double zeros at p_l, p_k . Therefore, $\tilde{x}(p)$ differs by a constant factor from the above normalized projection:

$$x(p) = \pm \frac{\theta^2[lkj35]}{\theta^2[skj35]} \frac{\theta^2[sk35](u(p))}{\theta^2[lk35](u(p))}, \quad k \neq s, l, j, \quad (5.7)$$

where the sign \pm in the latter formula depends on the parity (+ even / - odd) of the scalar product $\varepsilon(j) \cdot (\varepsilon'(s) + \varepsilon'(l))$, where the integer theta characteristic $[\varepsilon(s), \varepsilon'(s)]$ corresponds to a half-period of $u(p_s)$. In the case $k = j$ the normalization has to use L'Hospital's rule and we get a slightly different factor.

Also, the standard normalization of the projection $x(p_\alpha) = -1$, $x(p_\beta) = 1$, $x(p_0) = \infty$ brings us to a slightly more awkward expression:

$$x(p) := \pm 2 \frac{\theta^2[\beta j 35](u^0)}{\theta^2[\alpha \beta j 35]} \frac{\theta^2[\alpha j 35](u(p))}{\prod_{\pm} \theta[j 35](u(p) \pm u^0)} - 1, \quad j \neq \alpha, \beta,$$

in which the sign in front of the fraction depends on the parity of the scalar product $\varepsilon(\beta) \cdot \varepsilon'(\alpha)$, where $\varepsilon(s), \varepsilon'(s)$ is the representation of the half-period $u(p_s)$ by an integer theta characteristic.

Remark 4. There also exist other representations for a two-sheeted projection onto the sphere, for example, the Grant-Jorgenson formula [13], [14] uses partial derivatives of the sigma function, a close relative of the theta.

5.4. Rosenhain formulae. Putting in the above formula (5.7) the half-periods corresponding to the branch points, we get the effectively computed expressions for the latter in terms of the period matrix. For instance, if we normalize the projection $x(p)$ as $x(p_1) = 0$, $x(p_2) = 1$, $x(p_6) = \infty$, then we get the following expressions for the remaining branch points in terms of theta constants:

$$x_3 = \frac{\theta^2 \begin{bmatrix} 0 & 0 \\ 0 & 0 \end{bmatrix} \theta^2 \begin{bmatrix} 0 & 0 \\ 0 & 1 \end{bmatrix}}{\theta^2 \begin{bmatrix} 0 & 1 \\ 0 & 0 \end{bmatrix} \theta^2 \begin{bmatrix} 0 & 1 \\ 0 & 1 \end{bmatrix}}, \quad x_4 = \frac{\theta^2 \begin{bmatrix} 0 & 0 \\ 0 & 1 \end{bmatrix} \theta^2 \begin{bmatrix} 1 & 0 \\ 1 & 0 \end{bmatrix}}{\theta^2 \begin{bmatrix} 0 & 1 \\ 0 & 0 \end{bmatrix} \theta^2 \begin{bmatrix} 1 & 1 \\ 1 & 1 \end{bmatrix}},$$

$$x_5 = \frac{\theta^2 \begin{bmatrix} 0 & 0 \\ 0 & 0 \end{bmatrix} \theta^2 \begin{bmatrix} 1 & 0 \\ 1 & 0 \end{bmatrix}}{\theta^2 \begin{bmatrix} 1 & 1 \\ 1 & 1 \end{bmatrix} \theta^2 \begin{bmatrix} 0 & 1 \\ 0 & 1 \end{bmatrix}}.$$
(5.8)

Choosing another normalization for the projection, we get certain expressions for the cross-ratios of the same set of branch points, for example,

$$1 - x_3 = -\frac{\theta^2 \begin{bmatrix} 1 & 0 \\ 0 & 0 \end{bmatrix} \theta^2 \begin{bmatrix} 1 & 0 \\ 0 & 1 \end{bmatrix}}{\theta^2 \begin{bmatrix} 0 & 1 \\ 0 & 0 \end{bmatrix} \theta^2 \begin{bmatrix} 0 & 1 \\ 0 & 1 \end{bmatrix}}, \quad 1 - x_4 = -\frac{\theta^2 \begin{bmatrix} 0 & 0 \\ 1 & 0 \end{bmatrix} \theta^2 \begin{bmatrix} 1 & 0 \\ 0 & 1 \end{bmatrix}}{\theta^2 \begin{bmatrix} 0 & 1 \\ 0 & 0 \end{bmatrix} \theta^2 \begin{bmatrix} 1 & 1 \\ 1 & 1 \end{bmatrix}},$$

$$1 - x_5 = -\frac{\theta^2 \begin{bmatrix} 0 & 0 \\ 1 & 0 \end{bmatrix} \theta^2 \begin{bmatrix} 1 & 0 \\ 0 & 0 \end{bmatrix}}{\theta^2 \begin{bmatrix} 1 & 1 \\ 1 & 1 \end{bmatrix} \theta^2 \begin{bmatrix} 0 & 1 \\ 0 & 1 \end{bmatrix}}.$$
(5.9)

Comparing (5.8) and (5.9), we get certain relations for the theta constants which are the consequences of the Riemann theta identities. The expressions for the branch points of genus two (hence hyperelliptic) curves in terms of theta constants appeared in Rosenhain's work [8].

Theorem 6 ([8]). *For a nonsingular genus-2 curve all the 10 even theta constants $\theta[\varepsilon, \varepsilon']$, $\varepsilon^t \cdot \varepsilon' \in 2\mathbb{Z}$, are distinct from zero.*

Proof. Choose three distinct branching points p_s, p_j, p_l on the curve. Since $p_s \neq Jp_j$, the function $\theta_e(p)$ does not vanish at $p = p_l$ when $e = u(p_s) + u(p_j) + K$. The value $\theta_e(p_l)$ vanishes simultaneously with the theta constant $\theta[sjl35]$. When the indices s, j, l vary in the set $\{1, 2, \dots, 6\}$, the theta characteristic $[sjl35]$ runs through all 10 even characteristics.

One component of the Humbert variety in the complex Siegel space of genus 2 is the locus where at least one of even theta constants vanishes. This is exactly the locus of Riemann matrices that are not the period matrices of any genus-two Riemann surface.

5.5. Third-kind Abelian integrals. On any Riemann surface there exist a unique Abelian differential of the third kind $dv_{r,q}$ with simple poles at two prescribed points $r \neq q$ only, residues $+1$ and -1 , respectively, and trivial periods

along all a -cycles. It has a certain physical meaning in terms of the flow of an inviscid incompressible fluid on the surface with a source at r and sink at q . Our approach to effective conformal mapping is based on the fact that the integral of this differential can be expressed in closed form.

Theorem 7 (Riemann). *Choose any point $s \in X$; then for any two points $r, q \neq J_s$ of the surface the representation*

$$v_{rq}(p) := \int_*^p dv_{rq} = \log \frac{\theta(e + u(p) - u(r))}{\theta(e + u(p) - u(q))} = \log \frac{\theta[\varepsilon, \varepsilon'](u(p) - u(r))}{\theta[\varepsilon, \varepsilon'](u(p) - u(q))} + \text{const} \quad (5.10)$$

holds, where the theta characteristic $[\varepsilon, \varepsilon']$ corresponds to the zero $e := -u(s) - K$ of the theta function (say, it may be any odd integer characteristic).

Proof. Consider the following function of the variable $p \in X$:

$$\exp(-v_{rq}(p)) \frac{\theta(e + u(p) - u(r))}{\theta(e + u(p) - u(q))}.$$

One checks that it is locally holomorphic on the surface: the theta function in the numerator vanishes at the points r and s , the denominator vanishes at q and s . Moreover, this function is single valued on the surface, provided that the branches for $u(r)$ and $u(q)$ in (5.10) are properly chosen (the integration path from r to the initial point p_1 and further to q may be deformed to one disjoint from the a - and b -cycles). To prove this we use the Riemann bilinear identity

$$\int_{b_j} dv_{rq} = 2\pi i \int_q^r du_j \quad (5.11)$$

and the transformation properties (5.3) of theta functions. Therefore, the function in question is a constant independent of p .

Example. The CS-integral in § 4.2.1 may be represented as follows:

$$w_{\alpha\beta}(p) = \log \frac{\theta[3](u(p) + u^0)}{\theta[3](u(p) - u^0)} + C_1 u_1(p) + C_2 u_2(p), \quad (5.12)$$

where $u(p) := (u_1(p), u_2(p))^t$, $u^0 := u(p_0)$ and the constants C_1, C_2 are obtained from the system of linear equations $dw_{\alpha\beta}(p_\gamma) = 0$ when $\gamma = \alpha, \beta$.

§ 6. Algorithm of conformal mapping

Based on the formulae of the previous section, we can propose the algorithm of conformal mapping of the heptagon to the half-plane and vice versa. First of all, given the heptagon we have to determine the corresponding point of the moduli space $\mathcal{M}_{2,1}\mathbb{R}_3$.

6.1. Auxiliary parameters. Given (related to side lengths) coordinates H_s of the heptagon, we have to determine seven real parameters: the imaginary part of the period matrix Ω , the image $u^0 := u(p_0)$ of the marked point p_0 in the Jacobian of

the curve, and the real 2-vector $C := (C_1, C_2)$. These parameters give a solution to a system of seven real equations:

$$d\theta[35](u, i\Omega) \wedge d\left(\log \frac{\theta[3](u + u^0, i\Omega)}{\theta[3](u - u^0, i\Omega)} + C \cdot u\right) = 0, \quad u = u(p_\alpha), u(p_\beta), \quad (6.1)$$

which means that the CS-differential $dw_{\alpha,\beta}$ has zeros at the points p_α and p_β ;

$$\theta[35](u^0, i\Omega) = 0, \quad (6.2)$$

which means that the point u^0 lies on the AJ-image of the curve in the Jacobian and finally

$$\begin{aligned} H_1 &= \frac{1}{2}(C_1\Omega_{11} + C_2\Omega_{12} + 2\pi(1 - 2u_1^0)), \\ H_2 &= \frac{1}{2}C_1, \\ H_4 &= -\frac{1}{2}C_2, \\ H_5 &= -\frac{1}{2}(C_1\Omega_{12} + C_2\Omega_{22} - 4\pi u_2^0), \end{aligned} \quad (6.3)$$

which specify the side lengths of the heptagon.

Lemma 5. *Let the side lengths H_1, H_2, \dots, H_5 satisfy the restrictions described in Lemma 1; then the system of seven equations (6.1)–(6.3) has a unique solution $\Omega, u^0, C \in \mathbb{R}^2$ in the domain determined by the inequalities*

$$0 < \Omega_{12} < \min(\Omega_{11}, \Omega_{22}), \quad 0 < u_s^0 < \frac{1}{2}, \quad s = 1, 2.$$

Proof. The existence and the uniqueness of the solution to (6.1)–(6.3) in the specified domain follows from the existence and the uniqueness (up to real projective transformations) of the conformal mapping of a given heptagon to the upper half-plane.

Remark 5. Essentially we have just three nonlinear equations to solve, which can be done by the Newton method with parametric continuation. Indeed, take any point (Ω, u_1^0) in the large moduli space. Then solving just one nonlinear equation (6.2) we get the whole vector $u^0 = (u_1^0, u_2^0)$, then solving two linear equations (6.1) we get the constants C and substituting the values Ω, u^0, C into the last four equations (6.3) we get the dimensions of the appropriate heptagon. So we have got the correspondence of two points: one in the space $\mathcal{P}_{\alpha,\beta}$ and another, in the space $\mathcal{M}_{2,1}\mathbb{R}_3$. Now, any given point in the heptagon space may be connected to the obtained one by a path of at most two linear segments. Those may be effectively lifted to the moduli space by the Newton method.

6.2. Mapping a heptagon to the half-plane. Suppose a point w^* lies in the normalized heptagon (that is, with the vertex $w_1 = i\pi$). This heptagon corresponds to a single point in the large moduli space, which defines a real symmetric matrix Ω and real 2-vectors u^0 and C as solutions of the auxiliary system (6.1)–(6.3).

Consider the system of two equations

$$\log \frac{\theta[3](u^* + u^0, i\Omega)}{\theta[3](u^* - u^0, i\Omega)} + C \cdot u^* = w^*, \quad \theta[35](u^*, i\Omega) = 0 \quad (6.4)$$

with respect to the unknown complex 2-vector u^* .

Lemma 6. *System (6.4) has a unique solution u^* with theta characteristic from the block $\begin{bmatrix} -I & I \\ -I & I \end{bmatrix}$.*

Proof. The CS-integral normalized by $w_{\alpha\beta}(p_1) = i\pi$ maps the upper half-plane $\mathbb{H}^+ \subset X$ one-to-one onto the selected normalized heptagon. In other words, the equation $w_{\alpha\beta}(p^*) = w^*$ has a unique solution $p^* \in \mathbb{H}^+$. We can also find a single-valued branch of the Abel-Jacobi map with normalization $u(p_1) = 0$ in the upper half-plane. By (5.12) and Theorem 5 the complex 2-vector $u^* := u(p^*)$ satisfies the system (6.4) and by Theorem 1 its theta characteristic lies in the specified block of the space \mathbb{C}^2 .

Remark 6. The CS-integral is multivalued on the surface, therefore the system of two equations (6.4) can have many solutions (for instance, this is clear from the reflection principle for conformal mappings). We use constraints on the theta characteristic to single out the unique solution.

Substituting the solution u^* into the right hand side of expression (5.7) we get the evaluation at the point w^* of the conformal mapping $x(w)$ of the heptagon to the half-plane with the normalization $w_s, w_j, w_l \rightarrow 0, 1, \infty$:

$$x^* = \frac{\theta^2[lkj35]}{\theta^2[skj35]} \frac{\theta^2[sk35](u^*)}{\theta^2[lk35](u^*)}, \quad k \neq s, l, j. \quad (6.5)$$

6.3. Mapping the half-plane to a heptagon. Conversely, given a point x^* in the upper half-plane we solve the system of two equations

$$\frac{\theta^2[lkj35]}{\theta^2[skj35]} \frac{\theta^2[sk35](u^*)}{\theta^2[lk35](u^*)} = x^*, \quad \theta[35](u^*) = 0 \quad (6.6)$$

with respect to a complex 2-vector u^* with characteristics from $\begin{bmatrix} -I & I \\ -I & I \end{bmatrix}$ and substitute this solution into the formula

$$\log \frac{\theta[3](u^* + u^0)}{\theta[3](u^* - u^0)} + C \cdot u^* := w^*, \quad (6.7)$$

to get the image of the point x^* in the normalized heptagon.

Appendix: asymptotic of periods

Now we evaluate the range of the second column of the period matrix Ω for a fixed first column. The first component of the Abel-Jacobi map takes the upper half-plane (embedded in the Riemann surface) to a rectangle of size $1/2 \times \Omega_{11}/2$ with horizontal slot on the height of Ω_{12} , see the left part of Fig. 4. The length l of the slot varies from 0 to $1/2$ and parametrizes all the surfaces with fixed first column of the period matrix.

Lemma 7. *The following asymptotic formulae hold:*

- 1) $\Omega_{22}(l) \rightarrow \infty$ as $l \rightarrow 0$;
- 2) $\Omega_{22}(l) \rightarrow \Omega_{12}$ as $l \rightarrow 1/2$.

Proof. 1) We map the cut rectangle onto the half-plane with normalization $x_3 = 0$, $x_4 = 1$, $x_6 = \infty$; then the remaining parameters x_1 , x_2 and x_5 depend on l and have finite limits as $l \rightarrow 0$: for example, $x_5(0) = 1$.

The second element of the basis of holomorphic forms on the curve has the form $du_2 = L(x) \frac{dx}{y}$, where $L(x)$ is a real linear function with negative zero (in the interval (x_2, x_3)). We find an estimate for $L(x_5)$:

$$\begin{aligned} \frac{1}{2} &= \int_{x_4}^{x_5} du_2 \leq |L(x_5)| \int_{x_4}^{x_5} \prod_{j=1}^5 |x - x_j|^{-1/2} dx \\ &\leq |L(x_5)| |x_3 - x_4|^{-3/2} \int_{x_4}^{x_5} \frac{dx}{\sqrt{(x - x_4)(x_5 - x)}} = \pi |L(x_5)|. \end{aligned}$$

Next we find an estimate for the period Ω_{22} :

$$\left| \frac{\Omega_{22}}{2} \right| = \left| \int_{x_5}^{x_6} du_2 \right| > |L(x_5)| \int_{x_5}^{x_6} \prod_{j=1}^5 |x - x_j|^{-1/2} dx > \frac{1}{2\pi} \int_{x_5}^{\infty} \frac{dx}{(x - x_1)^{3/2}(x - x_4)}.$$

The last integral diverges at a logarithmic rate as $x_5(l) \rightarrow 1 = x_4$ as $l \rightarrow 0$.

2) Now we normalize the map of the cut rectangle on the half-plane by the conditions $x_2 = \infty$, $x_3 = 0$, and $x_4 = 1$. The remaining three points $1 < x_5 < x_6 < x_1$ are functions of the length l of the slit and have a common limit $x_{561} > 1$ as $l \rightarrow 1/2$. As previously, $du_2 = L(x) \frac{dx}{y}$, where $L(x)$ is a linear function with negative zero. Now we find an estimate for $L(x_4)$:

$$\begin{aligned} \frac{1}{2} &= \int_{x_4}^{x_5} du_2 \geq |L(x_4)| \int_{x_4}^{x_5} \prod_{2 \neq j=1}^6 |x - x_j|^{-1/2} dx \\ &\geq \frac{|L(x_4)|}{(x_5 - x_3)(x_5 - x_4)} \int_{x_4}^{x_5} \frac{dx}{(x_1 - x)^{3/2}}. \end{aligned}$$

Since x_1 and x_5 have the same limit as $l \rightarrow 1/2$, the last integral in this estimate diverges in the limit. Hence $L(x_4) \rightarrow 0$. Now we estimate the difference between Ω_{22} and Ω_{21} :

$$\frac{1}{2} |\Omega_{22} - \Omega_{21}| = \left| \int_{x_3}^{x_4} du_2 \right| \leq \frac{|L(x_4)|}{|x_5 - 1|^{3/2}} \int_0^1 \frac{dx}{\sqrt{x(1-x)}} \rightarrow 0.$$

Bibliography

- [1] T. A. Driscoll and L. N. Trefethen, *Schwarz-Christoffel mapping*, Cambridge Monogr. Appl. Comput. Math., vol. 8, Cambridge Univ. Press, Cambridge 2002.
- [2] A. Bogatyrev, M. Hassner and D. Yarmolich, "An exact analytical-expression for the read sensor signal in magnetic data storage channels", *Error-correcting codes, finite geometries and cryptography* (Toronto, ON, Canada 2007), Contemp. Math., vol. 523, Amer. Math. Soc., Providence, RI 2010, pp. 155–160.

- [3] B. Deconinck, M. Heil, A. Bobenko, M. van Hoeij and M. Schmies, “Computing Riemann theta functions”, *Math. Comp.* **73**:247 (2004), 1417–1442.
- [4] H. M. Farkas and I. Kra, *Riemann surfaces*, Grad. Texts in Math., vol. 71, Springer-Verlag, New York–Berlin 1980.
- [5] S. M. Natanzon, *Moduli of Riemann surfaces, real algebraic curves, and their superanalogs*, Moscow Center for Continuous Mathematical Education, Moscow 2003; English transl., Transl. Math. Monogr., vol. 225, Amer. Math. Soc., Providence, RI 2004.
- [6] A. Lebowitz, “Handle removal on a compact Riemann surface of genus 2”, *Israel J. Math.* **15**:2 (1973), 189–192.
- [7] A. Lebowitz, “Degeneration of a compact Riemann surface of genus 2”, *Israel J. Math.* **12**:3 (1972), 223–236.
- [8] G. Rosenhain, “Abhandlung über die Funktionen zweier Variabeln mit Vier perioden”, *Mem. Pres. l’Acad. de Sci. de France des savants* XI, 1851.
- [9] B. A. Dubrovin, “Theta functions and non-linear equations”, *Uspekhi Mat. Nauk* **36**:2 (1981), 11–80; English transl. in *Russian Math. Surveys* **36**:2 (1981), 11–92.
- [10] A. B. Bogatyrev, “Effective approach to least deviation problems”, *Mat. Sb.* **193**:12 (2002), 21–40; English transl. in *Sb. Math.* **193**:12 (2002), 1749–1769.
- [11] H. E. Rauch and H. M. Farkas, *Theta functions with applications to Riemann surfaces*, Williams & Wilkins, Baltimore 1974.
- [12] D. Mumford, *Tata lectures on theta*. I, Progr. Math., vol. 28, Birkhäuser, Boston, MA 1983; II, Progr. Math., vol. 43, Birkhäuser, Boston, MA 1984.
- [13] D. Grant, “Formal groups in genus two”, *J. Reine Angew. Math.* **411** (96–121).
- [14] J. Jorgenson, “On directional derivatives of the theta function along its divisor”, *Israel J. Math.* **77**:3 (1992), 273–284.

A. B. Bogatyrev

Institute for Numerical Mathematics,
Russian Academy of Sciences, Moscow;
Moscow Institute of Physics and Technology
(State University);
Faculty of Mechanics and Mathematics,
Moscow State University
E-mail: gourmet@inm.ras.ru

Received 22/NOV/11

Translated by A. BOGATYREV